A statistical analysis of satellite data of wave parameters in the Mediterranean and Norther Atlantic Ocean
-
a COMKISS report

Anastasia Baxevani, Georg Lindgren, Igor Rychlik and Laurence Tual

Mathematical statistics
Centre for Mathematical Sciences
Lund university

September 2000

Chapter 1

Introduction

One of the objectives of the EU-supported project COMKISS, *Conveying Metocean Knowledge Improvements onto Shipping Safety*, is to model the wave climate along selected shipping routes as it is observed and recorded in available satellite data, and thereby to identify possible local and seasonal variations, not available in wave statistics data bases.

The statistical study was aimed as input to the parts of the COMKISS project dealing with design criteria and fail safe conditions.

One goal set up, was to demonstrate the possible improvements in the definition of the loads to be taken into account for design rules in shipbuilding. Conventional strength criteria for ships are based on description of loads that is independent of actual ship service and corresponds to worst sea conditions expected over a period of 20 years. Knowledge of actual sea conditions would allow to demonstrate the capacity of a ship designed for a specific service.

A second topic has been to investigate the possible spatial structure of the wave climate, in particular the dependence structure over extended areas, in order to make possible the estimation of the fail-safe properties of ocean crossings, in particular to find the distribution of the worst wave conditions over a fixed period of time, typically 10-15 days.

The study was broken up in two parts. A Mediterranean route *Trieste - Rotterdam* was chosen for the design rules and an Atlantic route *Rotterdam - Boston* for the Fail safe part. The two routes are not only different from a meteorological point of view, but they are also monitored by the satellite passages in quite two different ways. The Mediterranean, in particular the Adriatic part near Trieste, is rather coastal near and there are many missing or unreliable data. The Atlantic data are rather reliable and stable. The parameters for the statistical distributions in the wave characteristics are of course different and varies along the route, small and regular variations in the Atlantic and large in the Mediterranean.

The main parameters studied are the significant wave height H_s and the zero-crossing period T_z. Data were altimeter Topex/Poseidon data from the WAVSAT archive at Satellite Observing Systems, Godalming.

Chapter 2

The Trieste - Rotterdam route

2.1 The data

The data are provided one per second of sea conditions from the TOPEX/Poseidon satellite, from Trieste to the Channel between October 1992 and January 1999. The route Trieste – Rotterdam, divided into 13 data regions, is depicted in Figure 2.1.

In Tual [2] it is checked that the H_s data in the Adriatic Sea follow a log-normal distribution. This also has to be checked for the rest of the data, particularly for the data in the Atlantic Ocean whose behavior might be different from the ones in the Adriatic (means of H_s for example are higher).

As illustrated through the two examples on Figure 2.2 where $\log(H_s)$ values are plotted on normal distribution paper, the log-normal distribution can also fit the data in the other parts of the route.

2.2 Time stratifications

As there is a major difference between winter and summer data, we separate the data and study the winter data (winter includes here October, November, December, January, February and March).

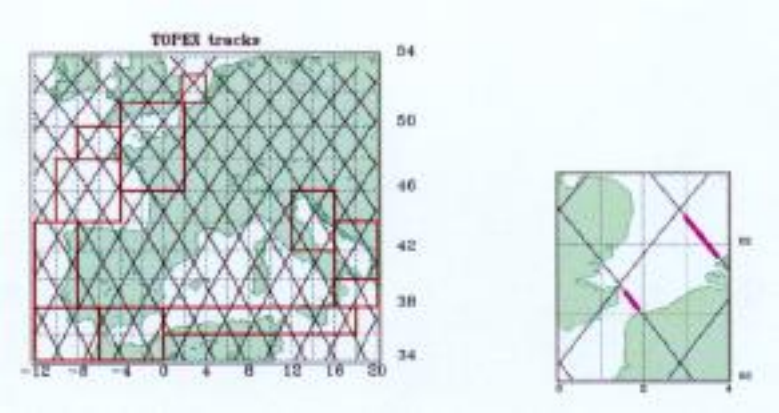

Figure 2.1: *Regions for extracted Topex altimeter data Trieste – Rotterdam.*

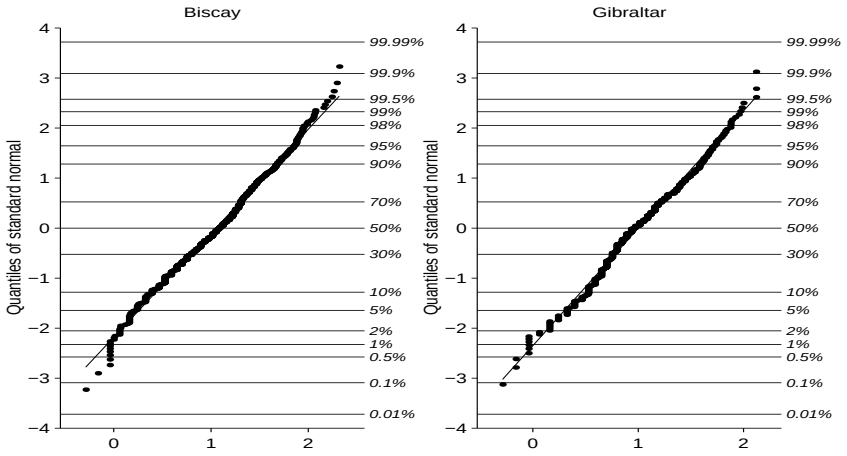

Figure 2.2: *Log-normal distributions for two examples : Biscay for H_s observations between $9^o W$ and $5^o W$ of longitude, and between $44^o N$ and $48^o N$ of latitude, Gibraltar for observations between $12^o W$ and $9^o W$ of longitude, and between $34^o N$ and $38^o N$ of latitude.*

2.3 Space selections

We select regions of about the size of a $2^o \times 2^o$ box so that the number of data along the part of the track included in this region is sufficient and the region selected is not too large and still satisfies homogeneity assumption. In each region we extract the data belonging to the same satellite track. Thus we get for, each track of each region, all the passages repeated every ten days. As there is no correlation from one passage to the next, ten days later, all the passages from the same track are considered as independent realizations of the space H_s process.

There are missing values for almost all the passages. These missing values were reconstructed following these steps:

Resampling: The positions, i.e. coordinates of longitude and latitude are re-discretized. As all the passages do not have the same number of observations and measurements are not made exactly at the same place from one passage to another, we have to re-organize it in order to make them comparable. We split the passages in as many small parts as possible. For all the passages we have the same number of equally spaced container (corresponding to the different *positions*). We create a matrix where the rows correspond to the positions and the columns to the different passages. Then we fill this matrix averaging all the $\log(H_s)$ values included in the same container. If no H_s value was observed at a given position and passage, it is filled by a missing datum.

Estimation: The autocovariance function was then estimated as follows. We first take away the mean of logarithmic values per passage in the previously obtained matrices. The auto-covariance function is then estimated for each passage and as all the passages are independent we take the mean of all the auto-covariances (in order to not give too much weight to the passages taken individually).

Interpolation: The H_s data are interpolated by two methods using the auto-covariance function:

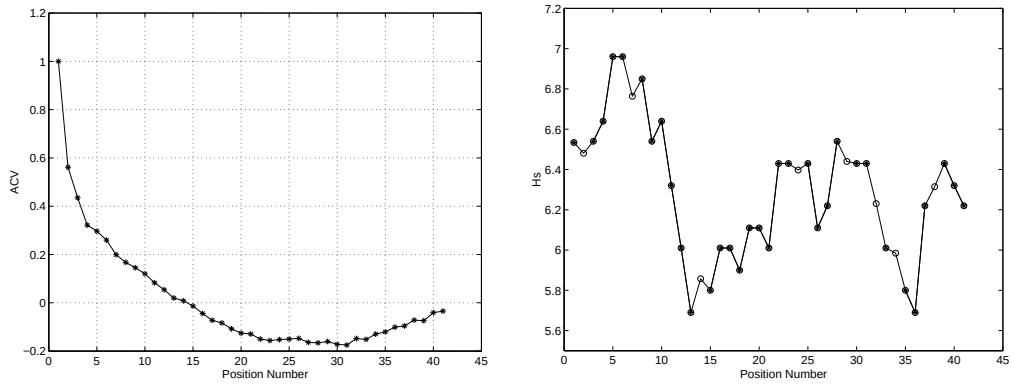

Figure 2.3: *Left: Estimation of the auto-covariance function (ACV) along a track; Right: Example of a reconstructed passage. The symbol o represents the reconstructed values and $*$ the non missing values before interpolations.*

one method uses the orthogonality principle for few missing values in a row. The other method uses simulation conditioned on the observed values under the specific assumption of a Gaussian random process, see Tual [2] for details.

We show an example of a reconstructed passage in the Atlantic Ocean. Figure 2.3 shows (left) the estimated auto-covariance function for this particular track and (right) an example of a passage along this track whose missing values have been replaced by this method.

2.4 Space variability of H_s during winter

For each window a unique log-normal distribution is fitted. Therefore we have two values per position i : the mean and standard deviation. Those values are smoothed giving estimates of the expectation of the logarithmic values $E[\log(H_s)]$ and the standard deviation $Std[\log(H_s)]$ per position along the passages and then they are extrapolated to the points between the tracks using cubic splines.

Figure 2.4 and Figure 2.5 show respectively the means m_i and standard deviations σ_i of the logarithmic values of H_s per position i on the whole extrapolated area.

We have estimated the 10% quantiles for H_s from this model. As the fractile corresponding to the probability 0.1 in a normal N(0,1) table is equal to 1.28, we get the H_s values corresponding to the 10% quantile using this formula : $z = \exp^{(m+1.28*\sigma)}$. These values are plotted on Figure 2.6.

Another way of getting the 10% quantile values is to use directly the reconstructed paths and select the values corresponding to the 10% quantile, smooth and extrapolate them the same way as it was done for means or standard deviations. These values are plotted on Figure 2.7.

The difference between them is the plotted of Figure 2.8, i.e. difference between H_s values corresponding to the 10% quantile in the log-normal model and H_s values corresponding to the 10% quantile from the reconstructed paths. As one can see on this figure, the difference is only noise. This enables to say that the model fits quite well the data everywhere.

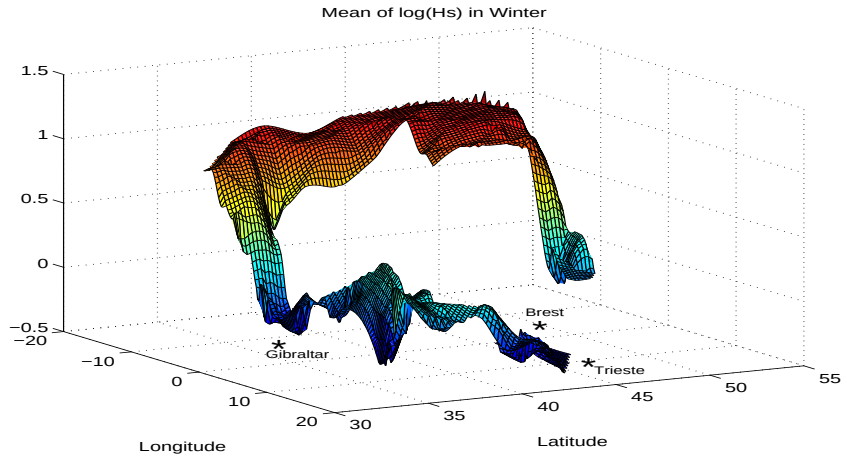

Figure 2.4: *Mean $E(\log H_s)$ per position*

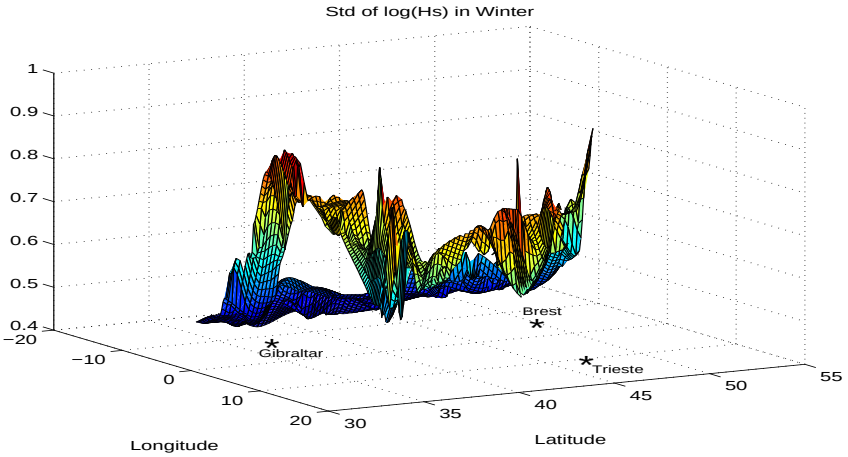

Figure 2.5: *Standard deviation $D(\log H_s)$ per position*

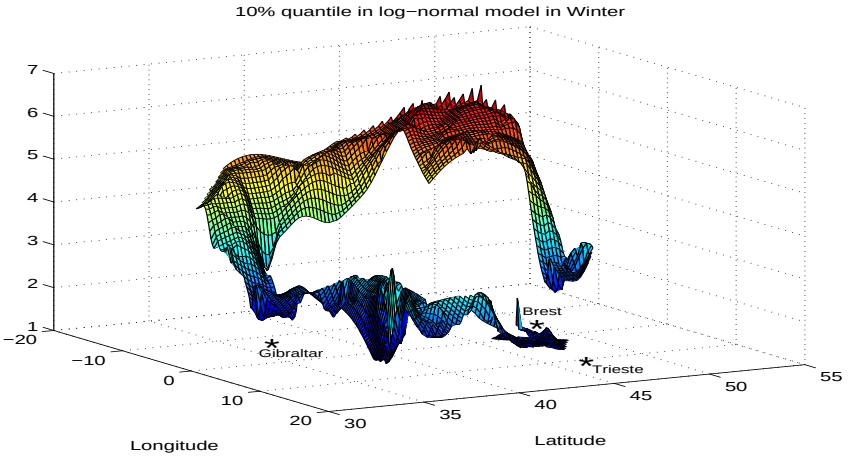

Figure 2.6: *10% Quantile values of H_s from log-normal model.*

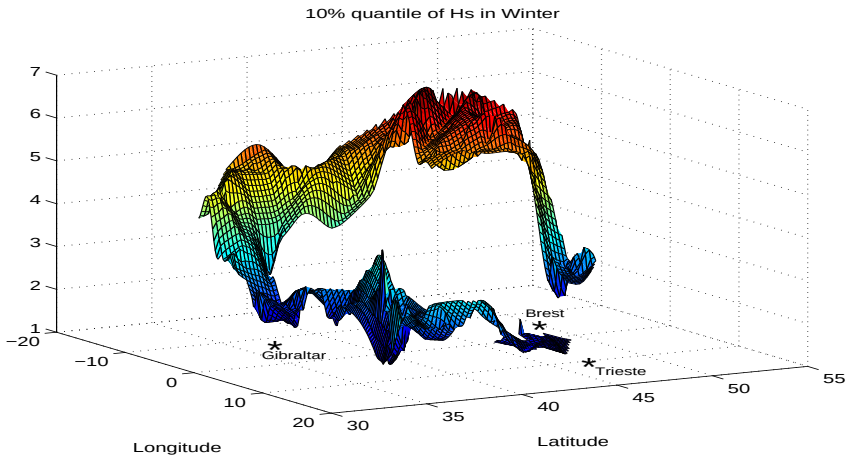

Figure 2.7: *10% Quantile H_s values computed directly from reconstructed paths.*

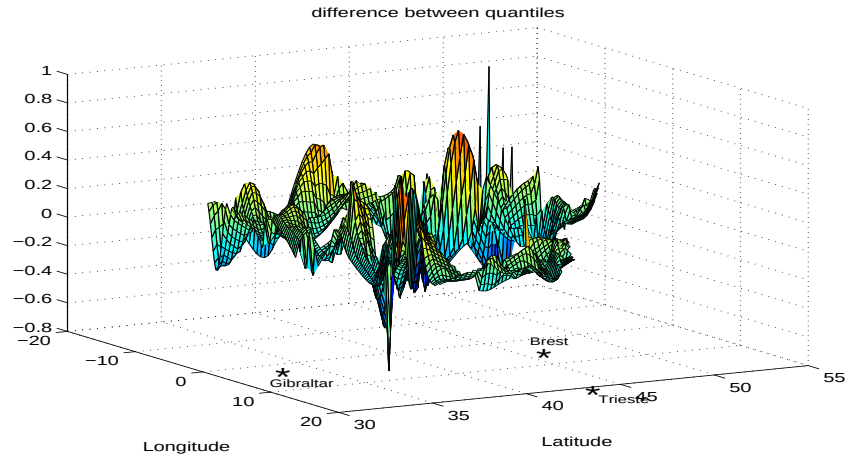

Figure 2.8: *Difference between H_s values corresponding to the two differently computed 10% quantiles.*

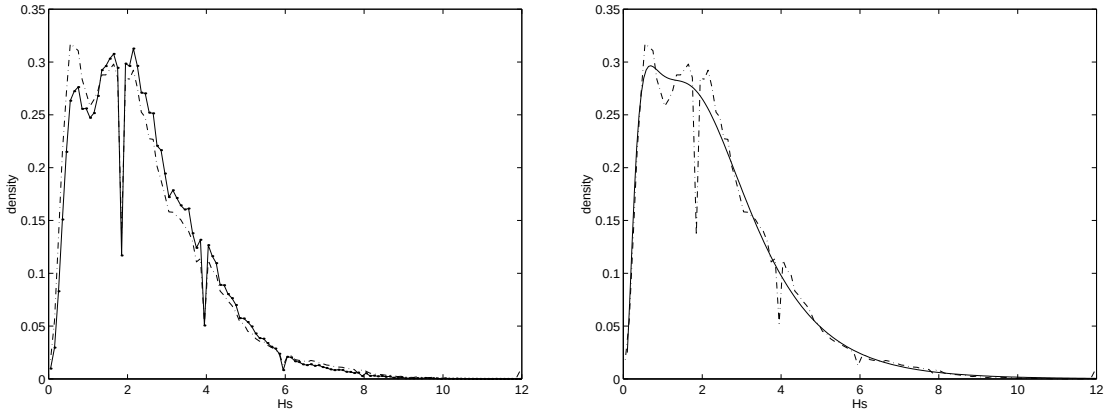

Figure 2.9: *Left: Densities of H_s. Solid line: before interpolation; dash-dotted line: after interpolation. Right:*

Densities of H_s. Solid lines: density function from the log-normal model ; dash-dotted line : from histogram of the interpolated data. Right: Densities of H_s on a particular route. Solid lines: density function from the log-normal model using non smoothed values; dash-dotted line: from density function from the log-normal model using smoothed values.

2.5 Validations

There are different methods and statistical processings that have to be checked or validated in this study. One has to know for example if it changes anything to use interpolated data or the original observations. One can also see if the extrapolated surface of smoothed means and standard deviations would differ if we used instead non smoothed values. Then it is important to validate the log-normal model. At last we compare density with smoothed or non smoothed values for a particular route.

2.5.1 Interpolated/Non interpolated data

To see the difference between interpolated data and the really observed values, we make histograms of them and compare their densities. This comparison is shown of Figure 2.9. We can see there are more low values once the data are interpolated (dash-dotted line). This is explained by the fact there is a correlation between low values and missing values (see Tual [2]), there is some bias introduced when these low values are missing. The down peaks observed on the figure for some particular values of H_s are surely due to the fact that the values are discretized.

2.5.2 Smoothed/non smoothed data

The means and standard deviations per position are smoothed on each passage before they are extrapolated on the whole surface. To see how this smoothing affects the values on the surface, we compare Figure 2.4 and Figure 2.5 with the means and standard deviations values computed without smoothing and shown respectively on Figure 2.10 and Figure 2.11. Comparing the figures, one can see there is not a big difference but for the data in Adriatic Sea. There, it is better to smooth

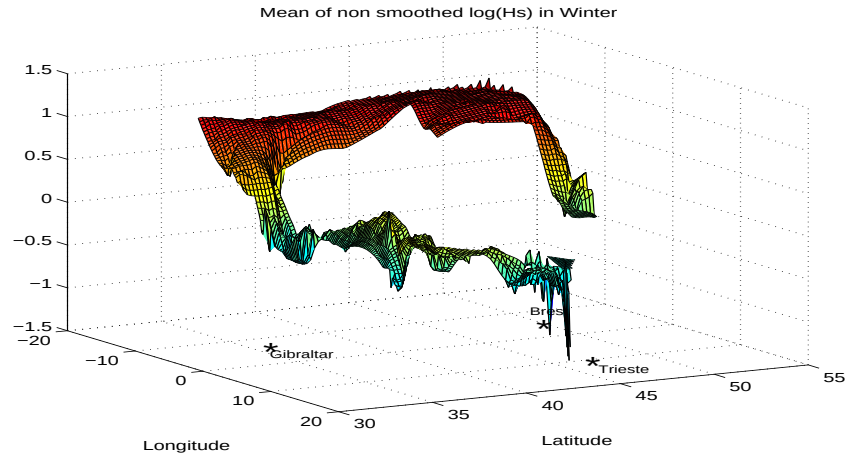

Figure 2.10: *Means of logarithmic values without smoothing*

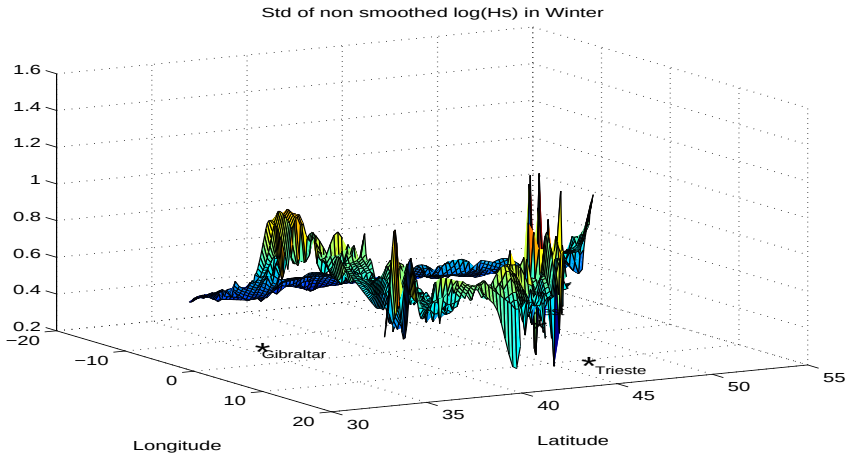

Figure 2.11: *Standard deviations of logarithmic values without smoothing*

the values but for the rest of the data it does not really matter.

2.5.3 Validation of the log-normal model

To validate the log-normal we compare the density obtained from the histogram of all observed H_s values, together with interpolated missing H_s values, with the density function as computed previously from the log-normal model (summing all the density functions at all positions along satellites tracks). This is shown in Figure 2.9, (right). One can see the log-normal model for this set of data is correct.

Chapter 3

The Rotterdam - Boston route

3.1 The data

The data consists of 629885 observations with 10 variables (Latidute, Longitude, H_s, Wind speed, T_z, minute, hour, day, month,year). Another variable called t (time) is also introduced, it is a transformation of the temporal variables, from minute to year into one variable. Readings are taken every second along the satellite's track corresponding to a spacing of about $7km$. Depending on the orbit height, the satellite will repeat the same pattern after a certain number of days. Records used in this study start on the 15^{th} of October 1992 and end on the 31^{st} of January 1999. Figures 3.1 and 3.2 show the westbound and eastbounds routes across the Atlantic and the different tracks of the satellite over the Atlantic Ocean, covering the routes.

Our main purpose in this chapter is to fit a model, similar to the one for the Trieste – Rotterdam route, to the distributions of both the significant wave height and the mean zero-crossing period. We would like to have a model for the probability density function (pdf) at any given location (lo,la) in the Atlantic.

Observations of the data along the different passages lead us to the conclusion that satellite passages are relatively short in comparison to the sizes of the storms. Therefore the space correlation is very high, however the signal is very noisy. This is in contrast to the Trieste – Rotterdam route where the correlation was almost zero after 50 hours.

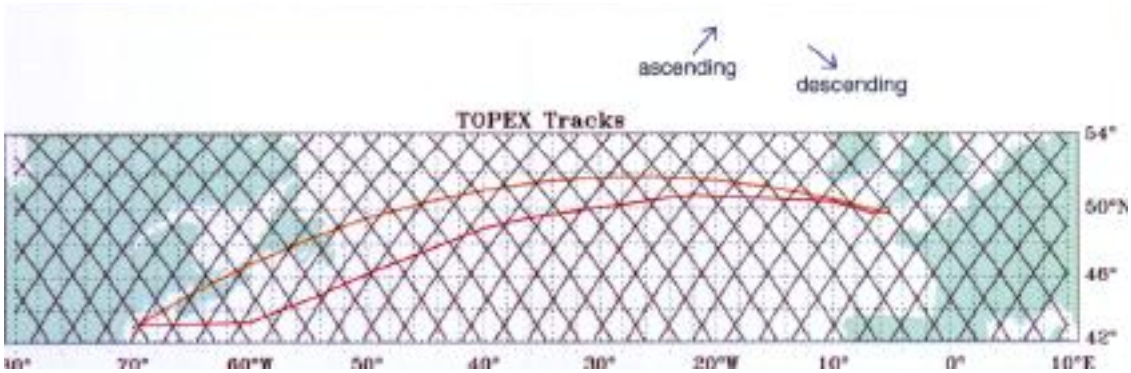

Figure 3.1: *Regions for extracted Topex altimeter data Rotterdam – Boston.*

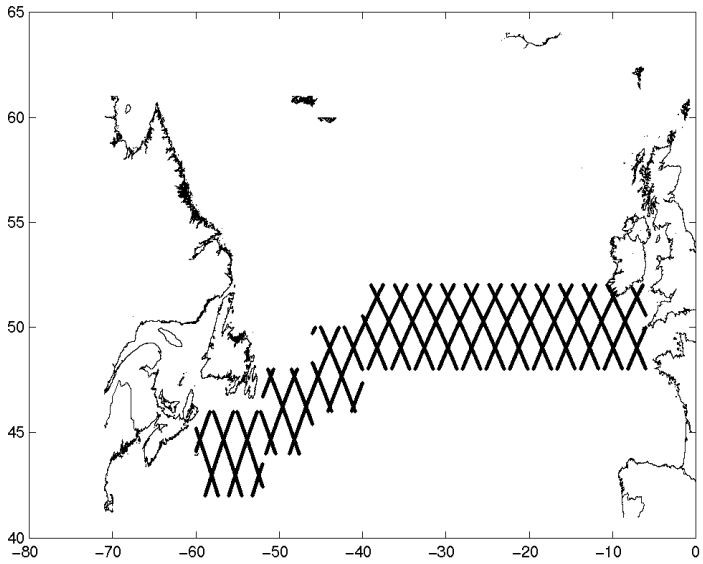

Figure 3.2: *Tracks of the satellite over the Atlantic.*

More analysis is required in order to have more precise statements about the spatial structure. The only space analysis we perform is computation of crossing intensities in the central part of the Atlantic. This part is homogeneous enough to allow the crossing intensity to provide us with information on the length of a cut of a line, like the route of a vessel, through a storm.

3.2 Wave height and zero-crossing period

3.2.1 Homogeneity and stationarity of the data

It is common knowledge that storms during winter are more frequent and more violent than those during summer. We selected January and February as representatives of winter and June and July for the summer. This choice is arbitrary. The same analysis could be performed for any other months. In what follows we use H_s to denote the significant wave height and T_z for the zero-crossing period.

We also made the valid assumption that the data along any latitude is almost homogeneous. Thereafter, we plotted H_s versus longitude for both winter and summer months. As seen in Figure 3.3, the H_s values are bigger in the middle of the Atlantic for both seasons. Moreover the regions of homogeneity appear to be large enough. More details on this subject will be given in the following subsection.

In Figure 3.4, H_s is plotted against time; "*" marks the end of a year. There are some indications of variability between the different years, but the short period covered by our data does not allow us to draw any valid conclusions at the moment.

3.2.2 Marginal Distributions

Under the assumption of stationarity in time and homogeneity in 2-dimensional space, we try to fit a parametric distribution to the significant wave height data.

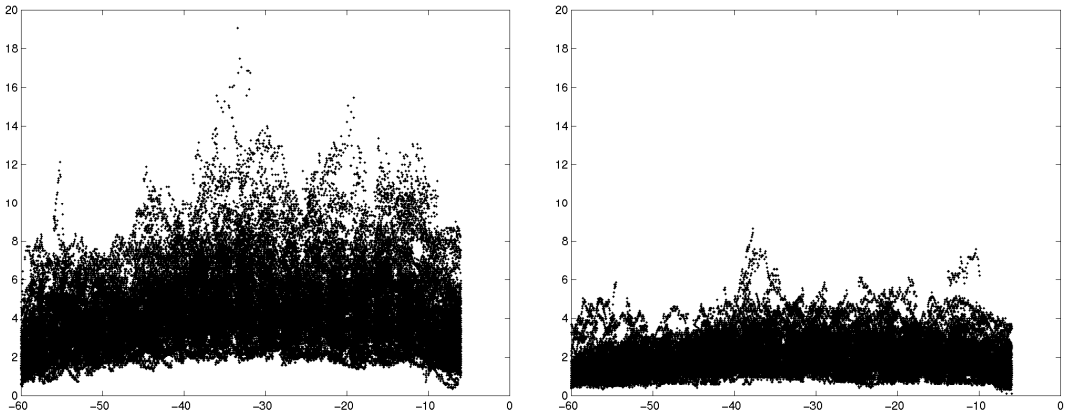

Figure 3.3: *H_s during 2 winter months vs longitude. H_s during 2 summer months vs longitude.*

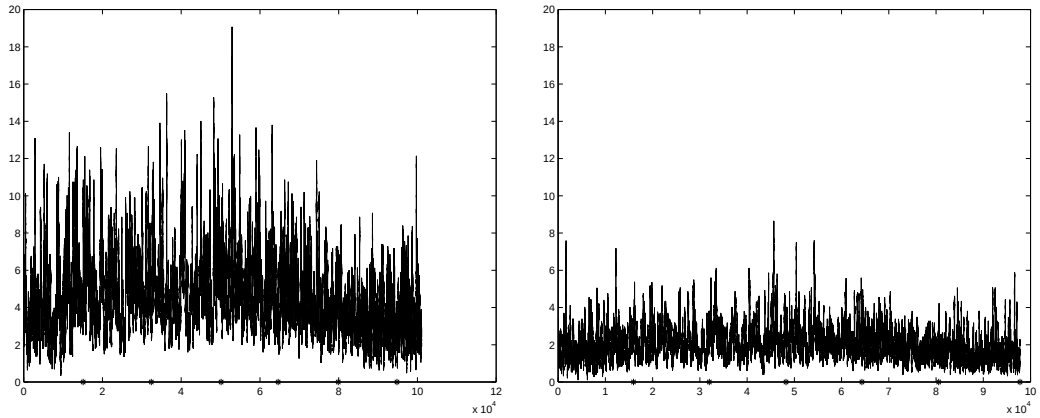

Figure 3.4: *H_s during 2 winter months. H_s during 2 summer months.*

The most commonly used distributions for such kind of data are Weibull distributions, Gumbel distributions, Gamma distributions and log normal distributions.

As we have already mentioned in the introduction, H_s is strongly correlated along the passages. Therefore, in trying to find a model for the distribution of H_s it is better to split the long passages we see in the middle of the Atlantic into smaller ones. We decided to separate them into north and south passages. We also face the problem of noise, data which oscillate around a slowly changing mean level. We deal with this by taking the mean value per passage. We have also extracted from each passage, the maximum and a fixed value (the third one). All of them they give a reasonably good fit to the log-normal distribution. The fits of the mean and the fixed point are almost equally good. The values for the maximum although obviously higher, still fit the log-normal distribution very well. The difference between the distribution for the maximum and the mean is of the order of 10 %.

The data we use in Figure 3.5 is from the area $[-44, -38] \times [46, 52]$ for the winter months, while in Figure 3.6 we use the data from the same area but for the summer months. The parameters μ and σ stand for the mean and standard deviation of $\log(H_s)$ respectively. As we see the data for the winter months do not come from the same distribution as those for the summer months.

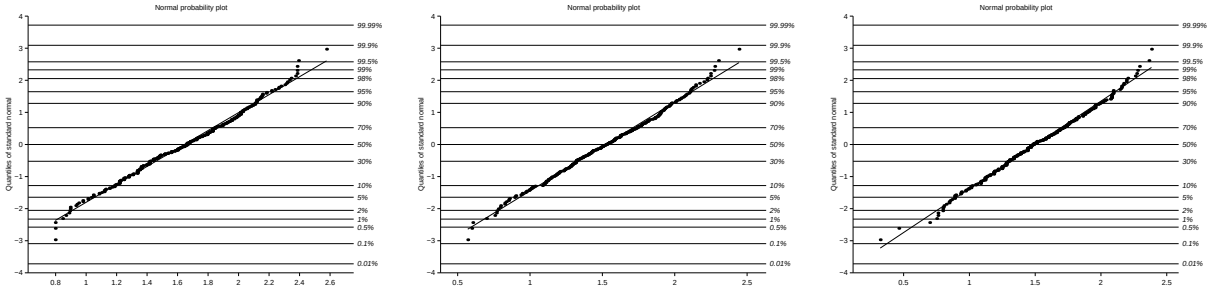

Figure 3.5: *log(max)/passage:* $\mu = 1.6447$, $\sigma = 0.359$, *log(mean)/passage:* $\mu = 1.5232$, $\sigma = 0.3618$, *log(fix)/passage:* $\mu = 1.5050$, $\sigma = 0.3670$, *plotted in normal probability paper.*

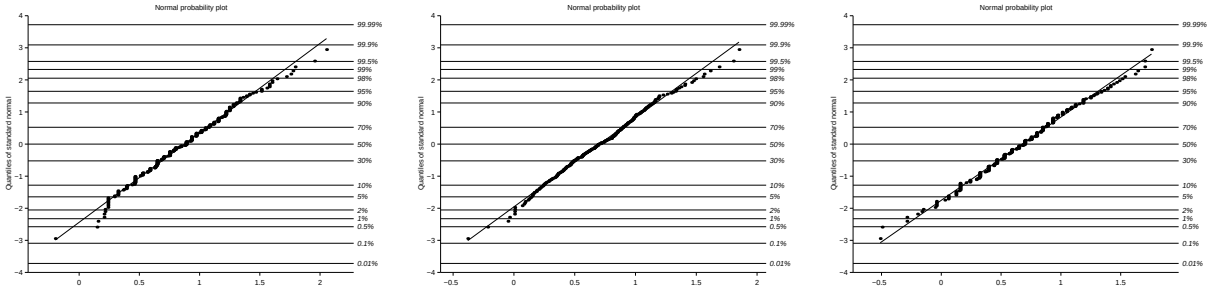

Figure 3.6: *log(max)/passage:* $\mu = 0.8745$, $\sigma = 0.3601$, *log(mean)/passage:* $\mu = 0.7054$, $\sigma = 0.3614$, *log(fix)/passage:* $\mu = 0.6758$, $\sigma = 0.3865$, *plotted in normal probability paper.*

The Figures 3.7 and 3.8 are from the area $[-44, -38] \times [50, 52]$, for winter and summer

respectively. As we can see in the figures the values for the parameters of the log-normal distribution in the smaller regions, are almost the same, which indicates homogeneity in the latitude direction.

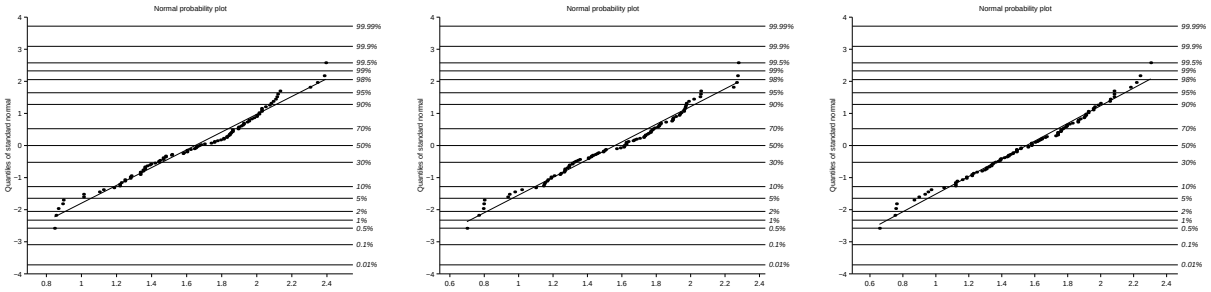

Figure 3.7: *log(max)/passage:* $\mu = 1.6483, \sigma = 0.3641$*, log(mean)/passage:* $\mu = 1.5596, \sigma = 0.3655$*, log(fix)/passage:* $\mu = 1.5493, \sigma = 0.3647$*, plotted in normal probability paper.*

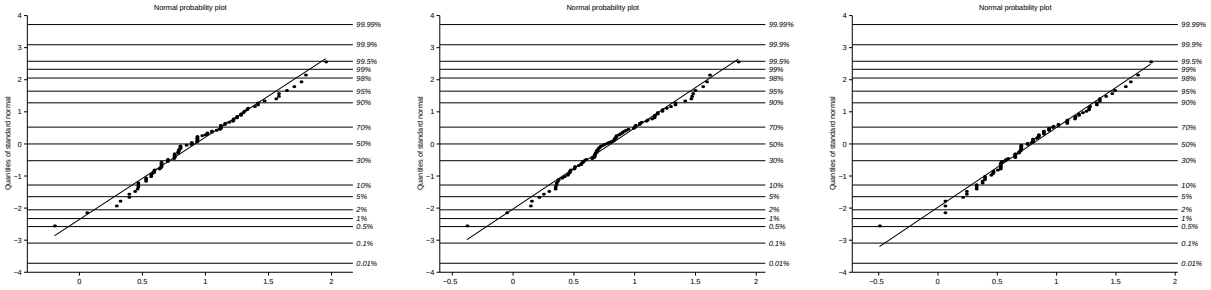

Figure 3.8: *log(max)/passage:* $\mu = 0.9180, \sigma = 0.3925$*, log(mean)/passage:* $\mu = 0.8035, \sigma = 0.3985$*, log(fix)/passage:* $\mu = 0.7931, \sigma = 0.4046$*, plotted in normal probability paper.*

3.2.3 Space Variability of H_s

We have already seen that the log-normal distribution fits reasonably well to the data extracted from various quite large regions. However in order to check for any dependencies between the parameters of the log-normal distributions and the space positions, we have split the area covered by the satellite into smaller areas of size $1^\circ \times 3^\circ$ or $2^\circ \times 3^\circ$. This allows us to assume homogeneity in space and at the same time it provides us with enough independent observations, around 70, per passage. This resulted into 40 regions for the summer months. However since in some of the areas we did not have enough data for the winter months, we had to combine some of these and got only 34 regions. For each window a unique log-normal distribution was fitted, which resulted into two values per position, the mean and the standard deviation for $\log H_s$. In Figures 3.9 and 3.10 we have plotted those values together with the lines we get from the non-parametric regression we performed.

In the area that extends between $[-45, -11]$ in longitude, it looks like the means come from almost the same distribution, an assessment that cannot be made for the rest of the regions. Moreover there is no reason for us to believe that the variability along the line is non-random. There is no evidence of a certain pattern. Sometimes the values from the northern areas are bigger than the ones from the south and sometimes exactly the opposite happens. This last observation leads us to believe that the variability is actually random and is mostly due to the variability of the latitude.

We have also checked the upper 10% quantile in the distribution of H_s for each region, both observed in the data and calculated from the fitted log-normal distributions, separated for winter and summer data. The results are shown in Figures 3.11 and Figures 3.12 for winter and summer data, respectively.

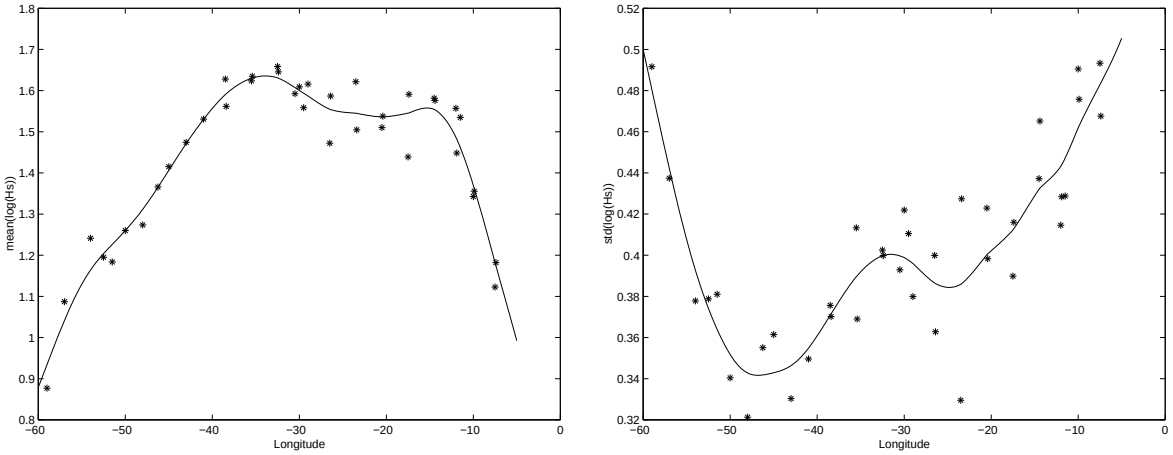

Figure 3.9: *Mean (left) and standard deviation (right) for* $\log H_s$ *during winter.*

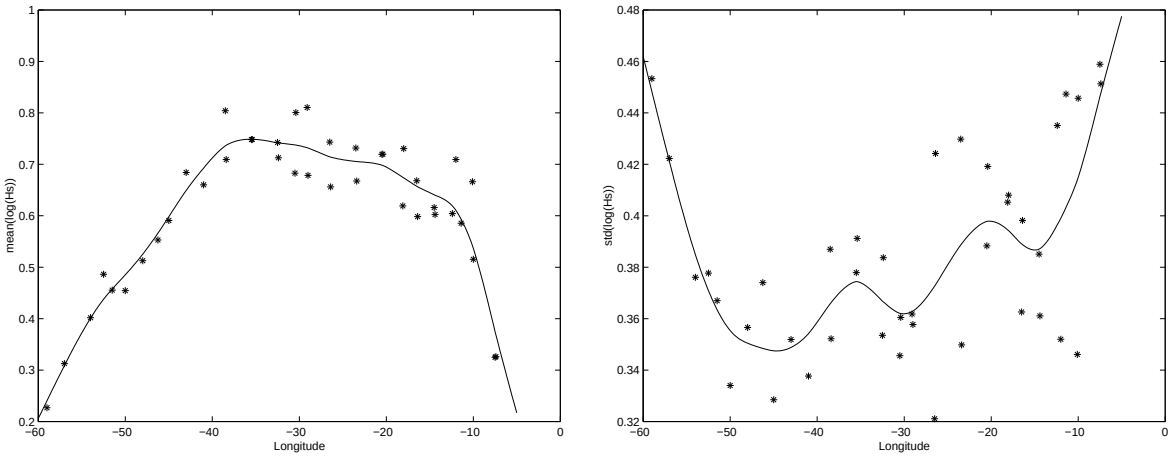

Figure 3.10: *Mean (left) for summer and standard deviation (right) for summer.*

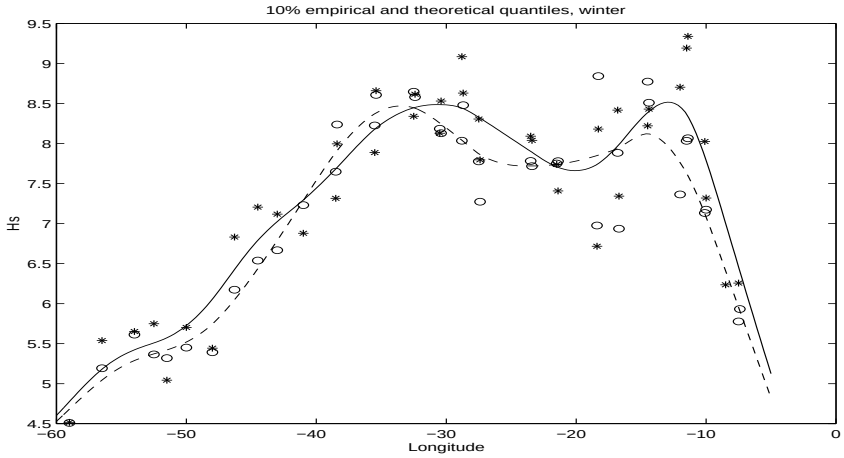

Figure 3.11: *10% Quantile values of H_s from empirical distribution (solid) and from log-normal distribution (dashed); winter.*

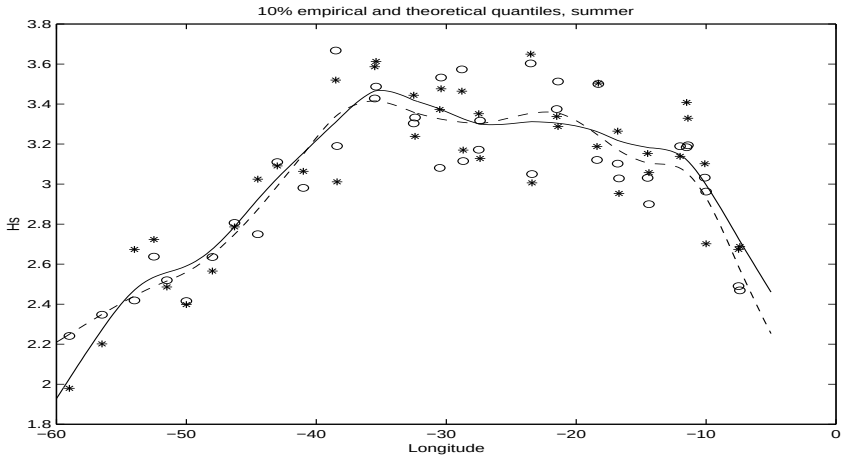

Figure 3.12: *10% Quantile values of H_s from empirical distribution (solid) and from log-normal distribution (dashed); summer.*

3.2.4 Joint Distribution of (H_s, T_z)

Besides the marginal distribution of the significant wave height, it may also be interesting to describe the joint distribution of H_s and T_z. The mean zero crossing period T_z, determines the number of cycles per unit (one cycle lasts T_z seconds on the average). It also helps to describe the different sea states since for example a small T_z value with a big H_s value would correspond to rough sea conditions. In Figure 3.13, T_z is plotted against H_s for the winter and summer data. It is obvious that T_z is a function of H_s. Here we have to mention that 315 observations have been removed from the data. These observations correspond to $T_z = 99.9$ and their occurrence varies between 3 (December) and 49 (June).

The conditional mean $E[\log T_z \mid \log H_s]$ was computed by linear regression – see the fit in

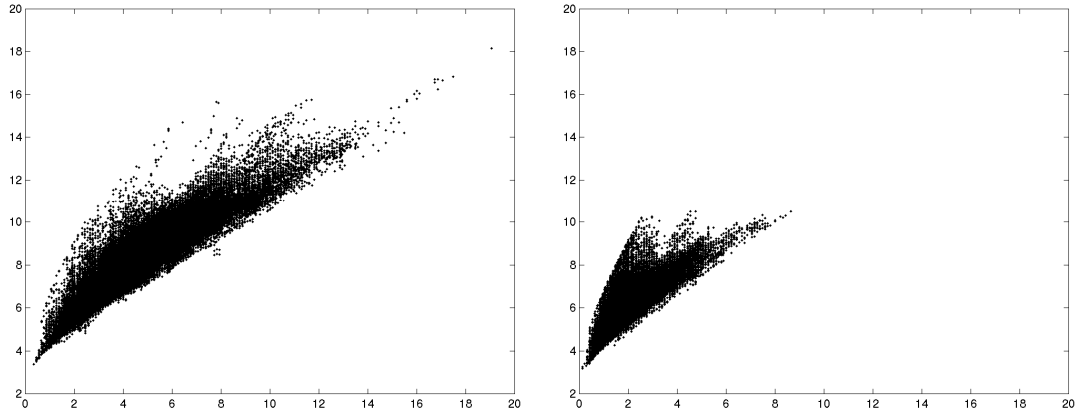

Figure 3.13: *Joint distribution of H_s and T_z for winter and summer.*

Figures 3.14. Then H_s is grouped in equally spaced 0.5-length classes, 29 for winter and 17 for the summer. In the winter data we grouped together the last 38 observations. This analysis gives us the regression line: $y = 0.4208x + 1.5047$, shown in Figure 3.14

The last class in the summer contains only one observation and is taken away in order not to disturb the regression. The result of this regression is $y = 0.3415x + 1.5750$. where y denotes $E[\log T_z \mid \log H_s]$ and x stands for the $\log H_s$ values. The dots in the plot are the actual

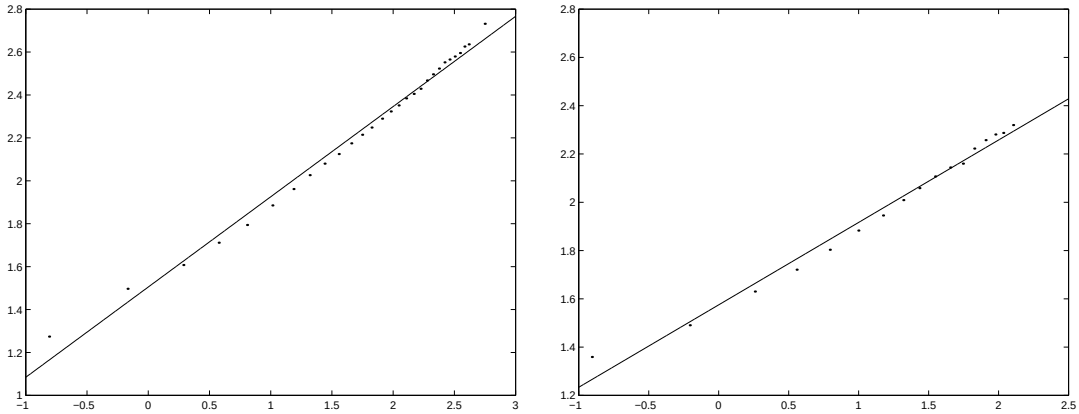

Figure 3.14: *Mean of* $\log T_z$ *as a function of* $\log H_s$ *for winter (left) and summer(right).*

measurements while the line is the result of the linear regression.

We have performed regression analysis on smaller areas and the results we obtained allowed us to conclude that a regression analysis on the whole data is useful. For example the area $[-34, -28] \times [48, 52]$ gives us $y = 0.4453x + 1.4345$ for the winter and $y = 0.3401x + 1.5365$ for the summer. These numbers are in accordance to the previous results.

Figures 3.15 and 3.16 show the conditional distributions of $\log T_z$ given $\log H_s$. In the first we have the log-normal plot of the conditional distribution of T_z for values of H_s in $[5, 5.5]$ and $[3.5, 4]$ for the summer months and in $[6, 6.5]$ and $[11, 11.5]$ for the winter months. The fit is not very good, but still useful for our analysis.

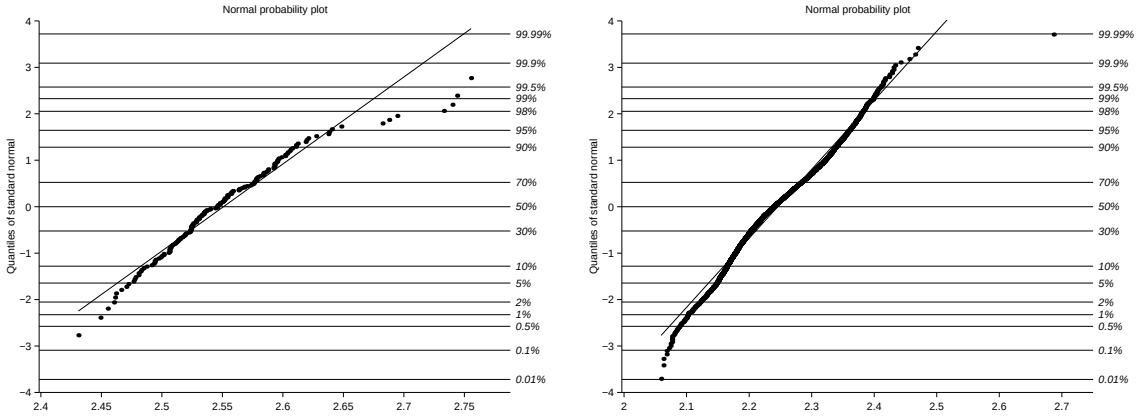

Figure 3.15: *Normal probability plots for* $\log T_z$ *for* H_s *in [11,11.5] (left) and [6,6.5] (right)*

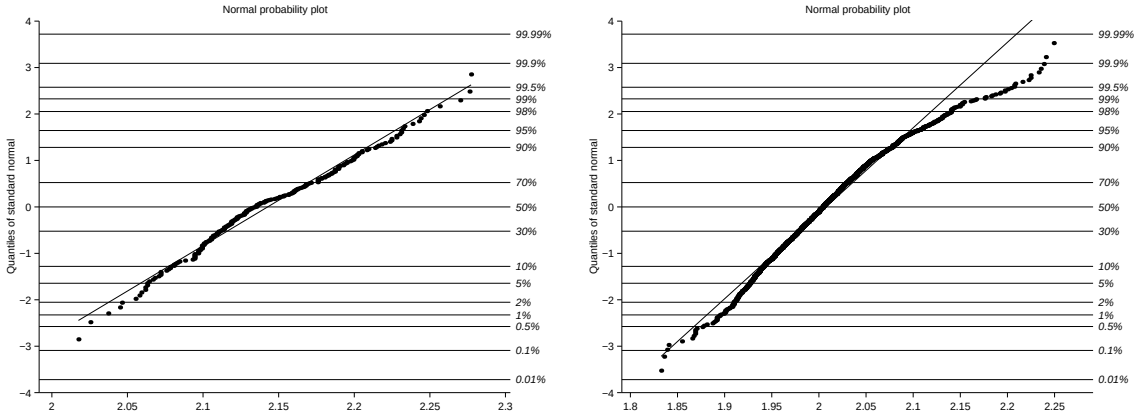

Figure 3.16: *Normal probability plots for* $\log T_z$ *for* H_s *in [5,5.5] (left) and [3.5,4] (right)*

3.3 Up-Crossings

In the previous section we have investigated the marginal distribution of H_s in the different geographical regions, where the wave parameters could be described as a homogeneous random field. The time stratification into winter and summer seasons was also done in order to asses the time stationarity of the field. We found that the log-normal distribution describes well the distribution of H_s at a fixed location and that the parameters of the distribution change slowly as one departs from the coast. The correlation of the field was not studied.

Since the log-normal distribution fits equally well at all locations a possible approach would be to model the field as a transformed Gaussian field. Studies from a fixed point (buoy) of time development of the H_s data give good support of such a model. In order to check the general validity of the transformed Gaussian field for the space and time variability of H_s we need data from many sources and larger coverage of the space by satellite. The region studied now is slightly too narrow. Research in this direction has been initiated.

The simplest approach seams to be to assume that the H_s in a region of homogeneity and under the period of stationarity is a transformed Gaussian field. Assuming such a model and that the speed of a vessel is constant the encountered H_s forms a non-stationary transformed Gaussian process (non-stationarity is caused by the inhomogeneity of the field in the scale of the whole route). The most important characteristics of this process is its crossing intensity of the encountered H_s process. The computation of this crossing intensity involves a kind of Doppler effect, since both the storms (and waves) and the vessel moves. The research on the means of computing the crossing intensity has been initiated.

Here we have analyzed a simpler problem. Assuming that we are considering the region of homogeneity, then the speed with which the satellite moves is much higher then the rate of changes of the H_s. Then measurements of H_s along a satellite track can be seen as a cut over the instantaneous weather condition. By estimating crossing intensities one can obtain an information of how often per [km] one is crossing a level, for example, significant wave height 8 meters. Using a transformed Gaussian model one can compute the average length of excursion above the level (space duration of the storm along a line) as well as an the approximation of the highest H_s during the excursion. More precise and detailed discussion of this problems will be given in a separate report.

We have checked crossings along two directions at the middle part of the Atlantic (that can be obtained from the satellite tracks) and did not find any differences in the crossing intensities, giving indications that sizes of excursions (storms) are in average independent of the direction of the path. This is clearly important if one wishes to use the information to analyze the size of storms along the route of a vessel.

We turn now to a short presentation of the estimated crossing intensity for one of regions of homogeneity. The crossing intensity is not easy to estimate, because the length of passages is short and the signals are noisy. Here we have used a property that for any fixed level, say h, the number of up-crossings of the level h is equal to the number of local maxima above the level h minus the number of local minima above h. Consequently by fitting suitable distributions to the observed local maxima and minima and taking the difference between them we obtain an estimate of the crossing intensity divided by the intensity of local maxima. In what follows we have a table for the parameters of the Gumbel distribution used for the local minima and local maxima distributions.

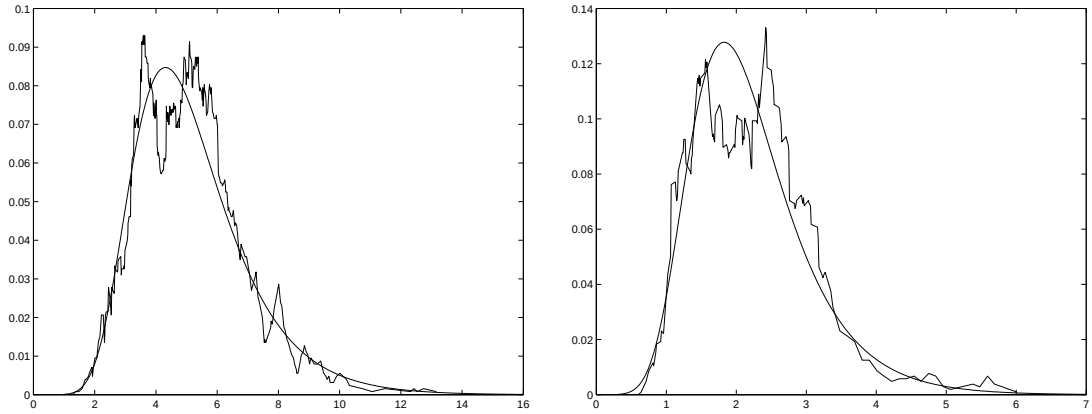

Figure 3.17: *Gumbel approx to number of upcrossings for winter and for summer.*

Table 3.1: *Parameters for Gumbel distribution.*

Area	Max-cycles	Min-cycles
1^{st} area winter	a=1.3757 b=1.3113	a=1.3113 b=3.8591
1^{st} area summer	a=0.6334 b=1.8589	a=0.6090 b=1.6436

3.4 Parameters for 40 regions

Table 3.2 contains the mean and the standard deviation of $\log H_s$ for 40 different regions for the months January and February. As we can see we have good fits in almost all the regions except from those close to either of the coasts.

In Figures 3.18-3.37 we have the plots for both log-normal and Weibull distributions for the forty areas. It is obvious that the log-normal distribution provides better fit for all the areas. We have also tested, although we have not included it in this appendix, the Gumbel distribution. This gave us the worst results. Hence we have concluded, that it is reasonable to assume that the data, in each small region, follow log-normal distributions and proceed with the rest of the analysis.

Table 3.2: *Parameters for Log-normal distribution for the months January and February. Distribution plots for the first two areas are found in Figure 3.18, for the third and fourth area in Figure 3.19, etc.*

Area	Mean	Standard Deviation
$[-40,-37]\times[50,52]$	1.5626	0.3686
$[-37,-34]\times[50,52]$	1.6349	0.3690
$[-34,-31]\times[50,52]$	1.6455	0.3998
$[-31,-30]\times[50,52]$	1.6159	0.3799
$[-30,-28]\times[50,52]$	1.6091	0.4129
$[-28,-25]\times[50,52]$	1.5868	0.3628
$[-25,-22]\times[50,52]$	1.5047	0.4274
$[-22,-19]\times[50,52]$	1.5378	0.3983
$[-19,-17.5]\times[50,52]$	1.6196	0.4374
$[-17.5,-16]\times[50,52]$	1.5611	0.3935
$[-16,-13]\times[50,52]$	1.5762	0.4652
$[-13,-11]\times[50,52]$	1.4483	0.4284
$[-11,-9]\times[50,52]$	1.3425	0.4905
$[-9,-6]\times[50,52]$	1.1225	0.4933
$[-40,-37]\times[48,50]$	1.6279	0.3756
$[-37,-34]\times[48,50]$	1.6237	0.4133
$[-34,-31]\times[48,50]$	1.6584	0.3837
$[-31,-30]\times[48,50]$	1.5925	0.3929
$[-30,-28]\times[48,50]$	1.5584	0.4105
$[-28,-25]\times[48,50]$	1.4822	0.3999
$[-25,-22]\times[48,50]$	1.6216	0.3295
$[-22,-19]\times[48,50]$	1.5101	0.4229
$[-19,-18]\times[48,50]$	1.4446	0.3890
$[-18,-16]\times[48,50]$	1.4333	0.3933
$[-16,-13]\times[48,50]$	1.5816	0.4372
$[-13,-12]\times[48,50]$	1.5569	0.4146
$[-12,-11]\times[48,50]$	1.5348	0.4288
$[-11,-9]\times[48,50]$	1.3555	0.4758
$[-9,-6]\times[48,50]$	1.1819	0.4676
$[-42,-40]\times[48,52]$	1.5307	0.3496
$[-44,-42]\times[48,52]$	1.4744	0.3303
$[-45,-44]\times[48,52]$	1.4151	0.3614
$[-47,-45]\times[48,52]$	1.3657	0.3551
$[-49,-47]\times[40,52]$	1.2736	0.3213
$[-51,-49]\times[40,52]$	1.2600	0.3404
$[-52,-51]\times[40,52]$	1.1836	0.3810
$[-53,-52]\times[40,52]$	1.1951	0.3788
$[-55,-53]\times[40,52]$	1.2413	0.3778
$[-58,-55]\times[40,52]$	1.0872	0.4374
$[-60,-58]\times[40,52]$	0.8769	0.4916

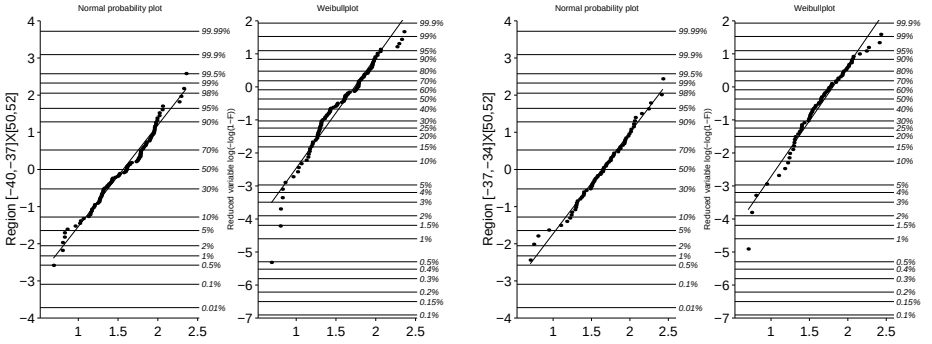

Figure 3.18: *Region 1, 2*

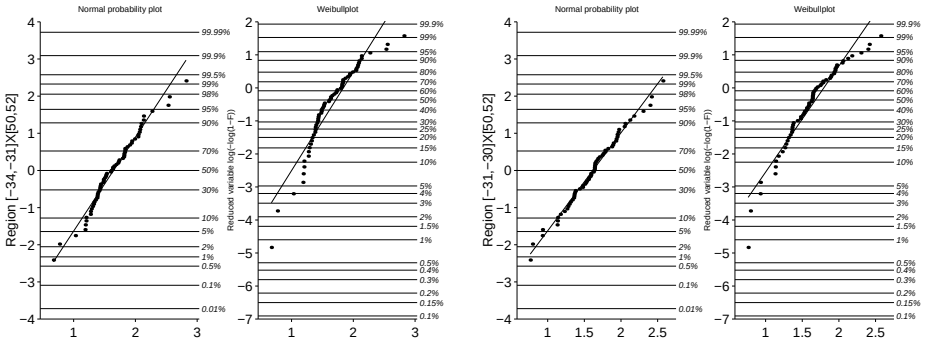

Figure 3.19: *Region 3, 4*

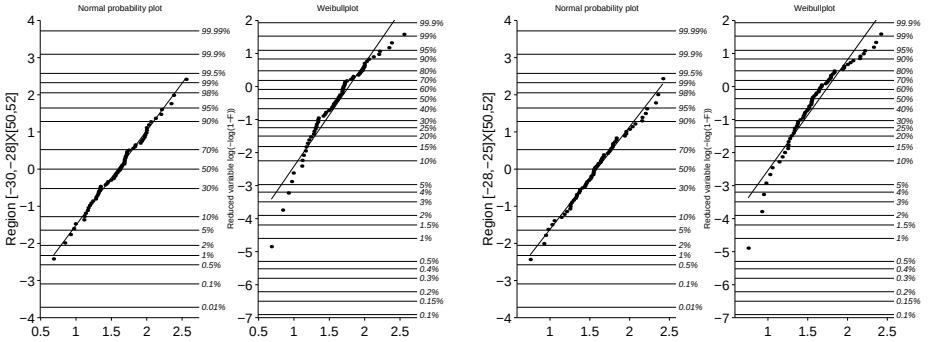

Figure 3.20: *Region 5, 6*

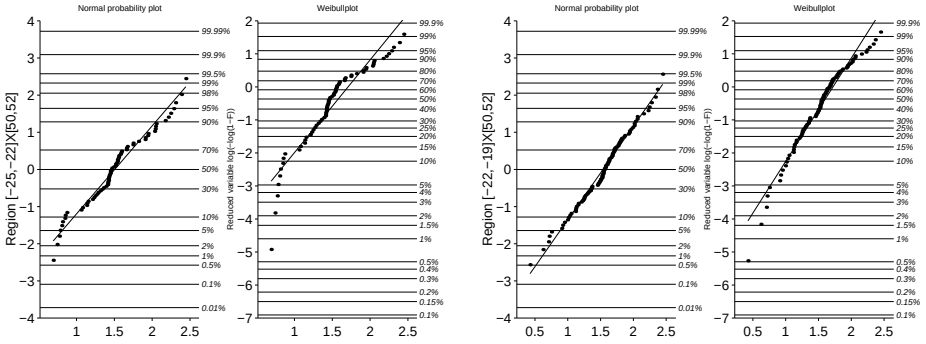

Figure 3.21: *Region 7, 8*

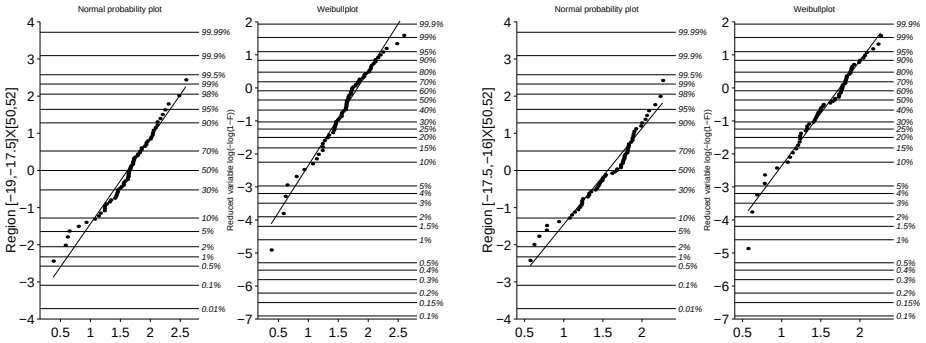

Figure 3.22: *Region 9, 10*

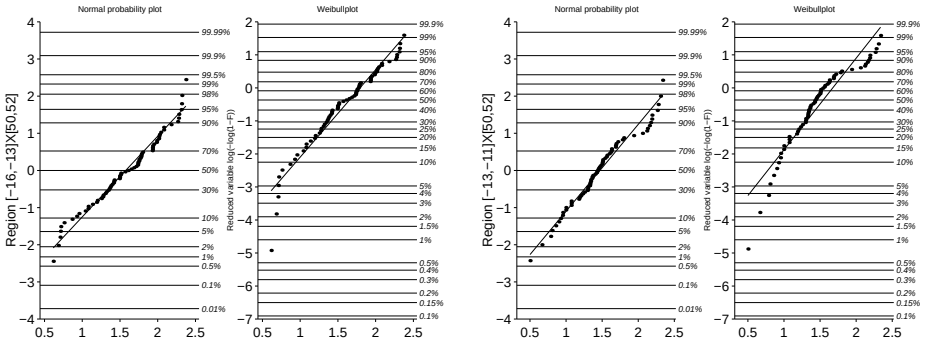

Figure 3.23: *Region 11, 12*

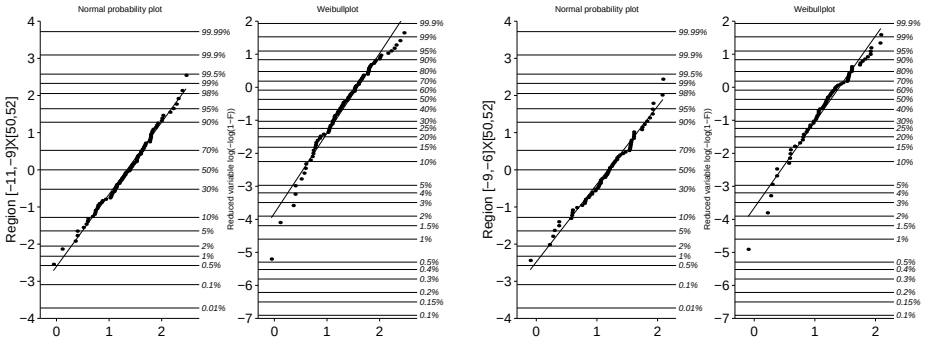

Figure 3.24: *Region 13, 14*

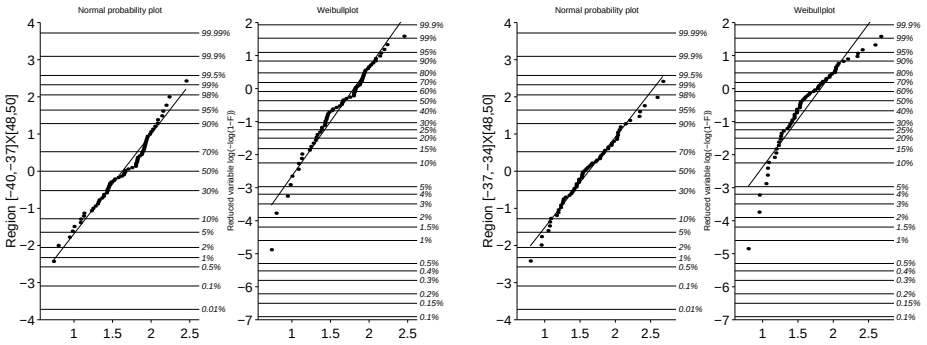

Figure 3.25: *Region 15, 16*

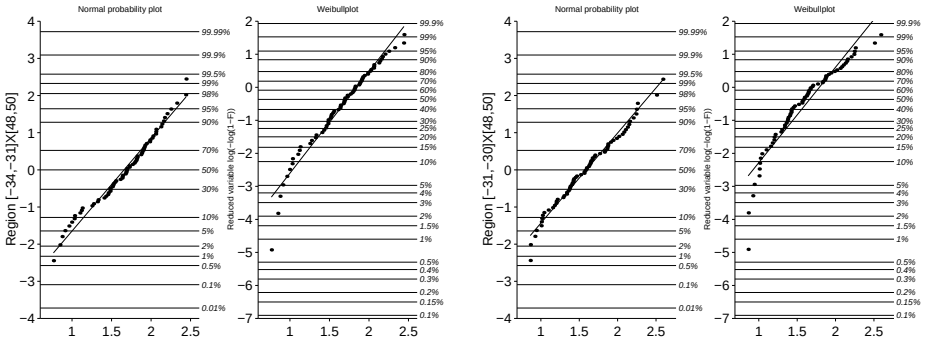

Figure 3.26: *Region 17, 18*

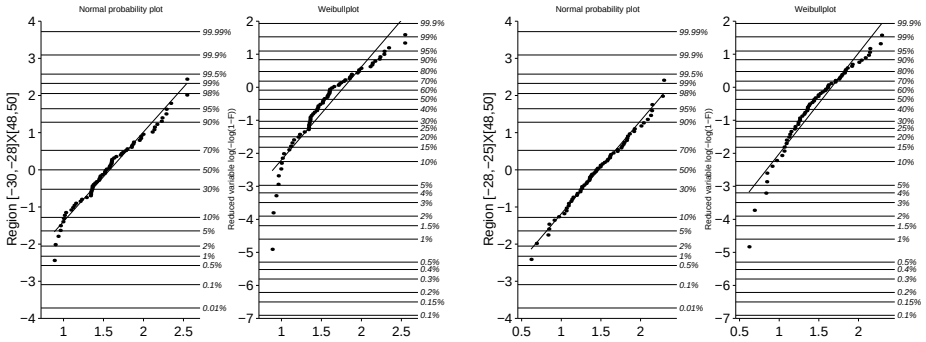

Figure 3.27: *Region 19, 20*

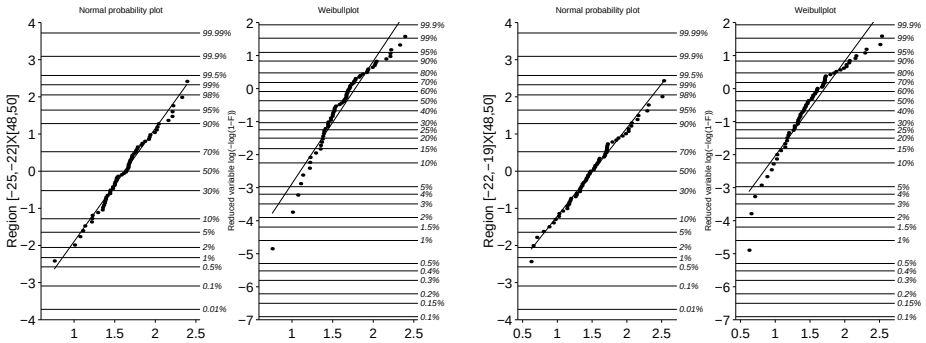

Figure 3.28: *Region 21, 22*

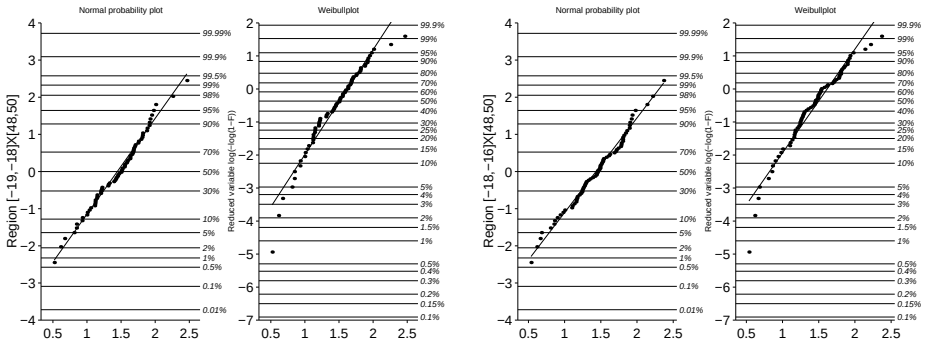

Figure 3.29: *Region 23, 24*

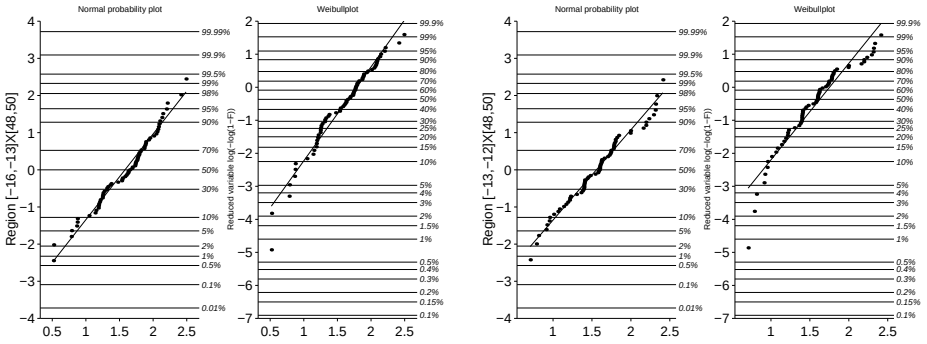

Figure 3.30: *Region 25, 26*

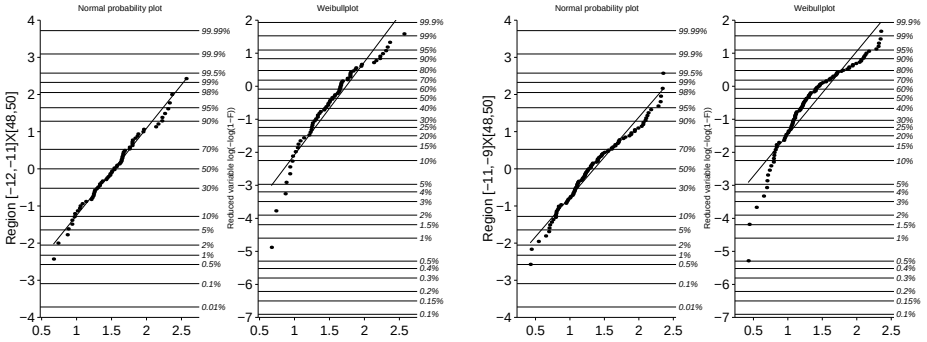

Figure 3.31: *Region 27, 28*

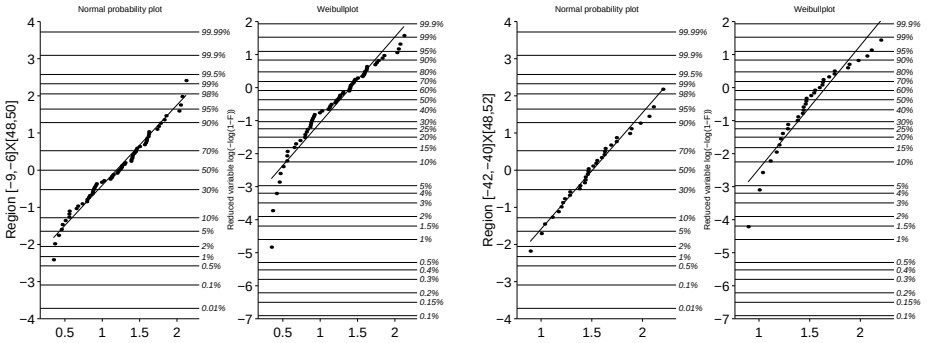

Figure 3.32: *Region 29, 30*

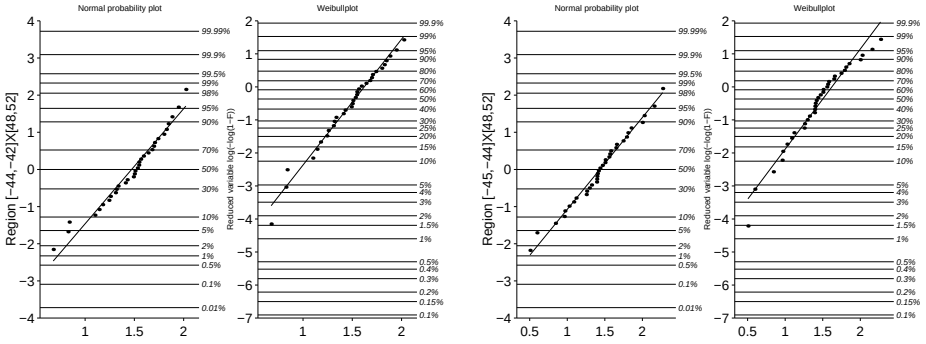

Figure 3.33: *Region 31, 32*

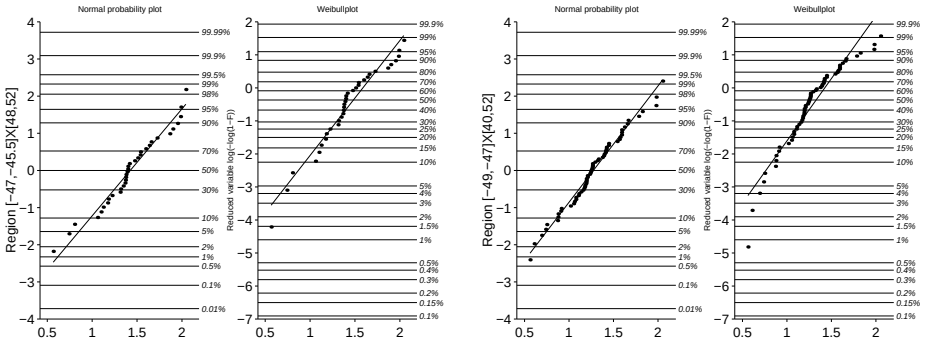

Figure 3.34: *Region 33, 34*

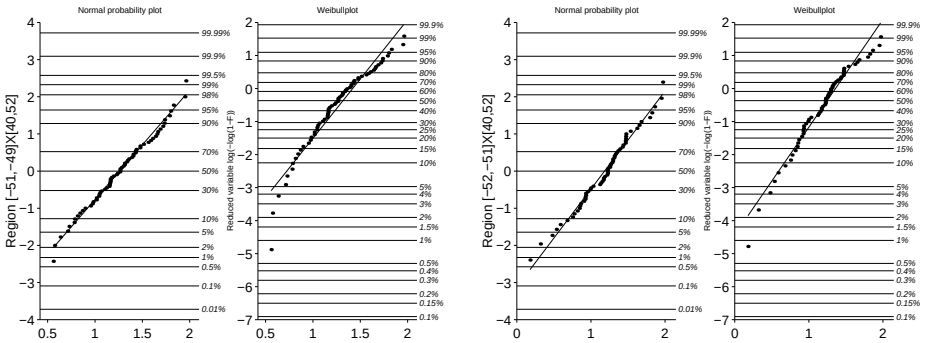

Figure 3.35: *Region 35, 36*

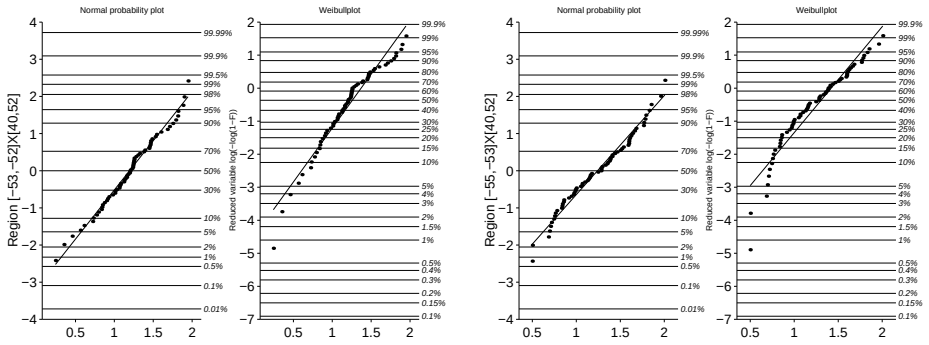

Figure 3.36: *Region 37, 38*

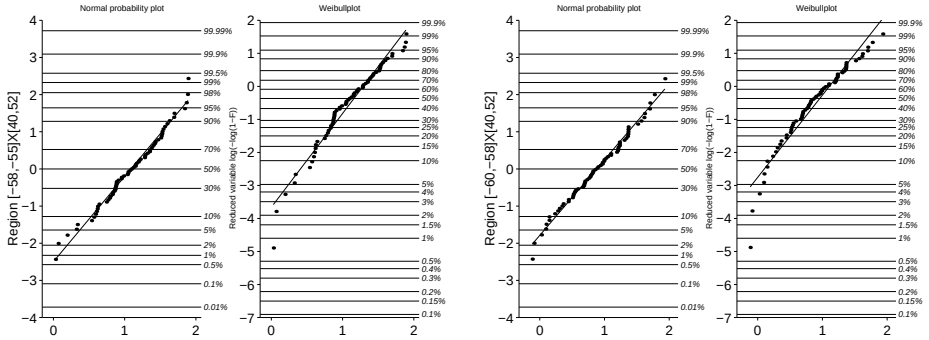

Figure 3.37: *region 39, 40*

Chapter 4

Encountered H_s during a voyage – fatigue assessment

4.1 Average fatigue damage

The average fatigue load experienced by a vessel on a particular route depends on the time it spends in each homogeneity zone of the wave characteristic distributions, in particular the H_s-distribution. The log-normal distribution was found to give an acceptable fit to this distribution in each region, with parameters varying only with location and time of the year. It is therefore easy to assess the total fatigue load for each trip.

Each route was divided into a number of homogeneous regions, and the log-normal parameters μ_i, σ_i, $i = 1, \ldots, N$, fitted to each region and season.

For the route from Rotterdam to Boston the absence of any evident non-homogeneity in the data, at least in the south-north direction, allows us to parameterize the route using only the longitude positions. The route was split into $N = 200$ different regions with parameters depending on longitude. For the Trieste - Rotterdam route we used $N = 160$ regions, with strong dependence on location along the route.

Each route was thus represented by a succession of N equally spaced nodes $N_i, i = 1, \ldots, N$. For each N_i along the route we evaluate both μ_i and σ_i, by means of interpolations of the mean and standard deviation values around the nodes. We also made the extra assumption of a constant speed and this is the reason the nodes are equally spaced, otherwise we were supposed to do the necessary adjustments.

The density function of H_s encountered by the boat along the route is given by:

$$f_H(h) = \frac{1}{N}\sum_{i=1}^{N} f_i(h),$$

where h denotes the H_s values. Inserting the density function for a log-normal variable h for each node, we get the H_s as

$$f_H(h) = \frac{1}{N}\sum_{i=1}^{N} f_i(h) = \frac{1}{N}\sum_{i=1}^{N} \frac{1}{h\sigma_i\sqrt{2\pi}} \exp\left\{-\frac{1}{2}\left(\frac{\log(h)-\mu_i}{\sigma_i}\right)^2\right\}. \tag{4.1}$$

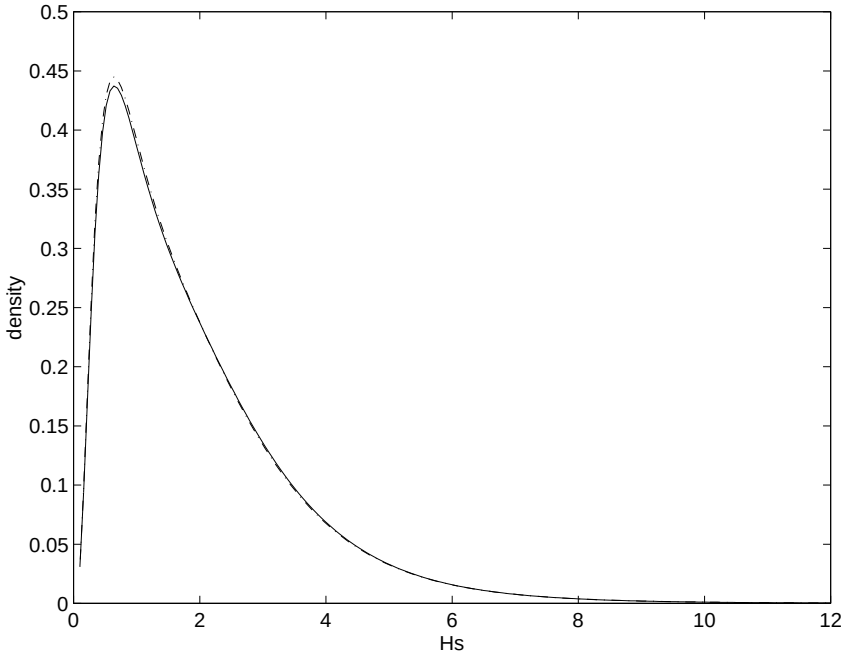

Figure 4.1: *Densities of H_s on a particular route. Solid lines: density function from the log-normal model using non smoothed values; dash-dotted line: from density function from the log-normal model using smoothed values*

4.2 Load distribution along the route

In previous chapters we have found log-normal distributions for all the different regions on the studied routes. These distributions can be merged for use in equation (4.1). We show the results for the two routes.

Figure 4.1 shows the density function for H_s along the route computed for the whole route of the boat either from smoothed or non smoothed mean and standard deviation values. There is a very slight difference. Therefore it will not affect much the fatigue damage computation whether one uses smoothed or non smoothed values for a route from Trieste to Rotterdam.

Figures 4.2 and 4.1 contain the densities for winter and summer period for the Rotterdam – Boston route.

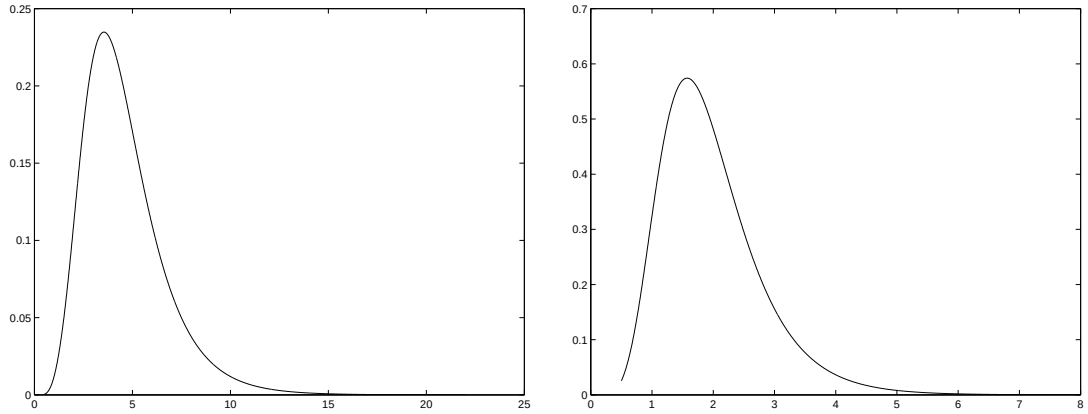

Figure 4.2: *Probability density of H_s for winter (left) and summer (right) for the Rotterdam – Boston route.*

Bibliography

[1] Baxevani, A., Podgórski, K. & Rychlik,I. (2000): *Distributions of responses experienced by a vessel*, Techn. Report, Lund Institute of Technology.

[2] Tual, L. (1999): *Wave Statistics on Satellite Measurements*, Master's Thesis, Lund Institute of Technology.